J. Nonlinear Var. Anal. 10 (2026), No. 5, pp. 927-940
Available online at http://jnva.biemdas.com
https://doi.org/10.23952/jnva.10.2026.5.04

MATHEMATICAL AND NUMERICAL SIMULATION USING A DEEP NEURAL NETWORK FOR A FRICTIONLESS CONTACT PROBLEM WITH UNILATERAL CONSTRAINTS IN VISCOELASTICITY

GUANGWANG SU[1], MUSTAPHA BOUALLALA[2], VAN THIEN NGUYEN[3], BOLING CHEN[4,*]

[1]*College of Artificial Intelligence, Nanning University, Nanning, China*
[2]*Modeling and Combinatorics Laboratory, Department of Mathematics and Computer Science, Polydisciplinary Faculty, Cadi Ayyad University, Safi, Morocco*
[3]*Department of Mathematics, FPT University, Hanoi, Vietnam*
[4]*Guangxi Colleges and Universities Key Laboratory of Complex System Optimization and Big Data Processing, School of Mathematics and Statistics, Yulin Normal University, Yulin, China*

Abstract. In this paper, we address a frictionless contact problem involving a viscoelastic body and an obstacle. The process is assumed to be quasi-static. The contact is modeled with normal compliance and unilateral stress, incorporating the Signorini contact condition. We derive a variational formulation of the model and demonstrate the existence and uniqueness of a weak solution using the theory of variational inequalities and fixed point arguments. By converting the initial contact problem into a minimization framework, we utilize a deep neural network to approximate the solution and address the minimization challenge. Finally, we provide numerical results that showcase the method's efficiency and precision.

Keywords. Deep neural networks; Elasticity; Frictionless contact problem; Unilateral constraints; Viscoelasticity.

1. INTRODUCTION

A contact problem arises when two or more bodies, not mechanically connected, come into contact without becoming rigidly attached to each other. This phenomenon is common in various industrial and everyday contexts, such as the contact between brake pads and wheels, tires and road surfaces, pistons and their skirts and so on. When one of the bodies involved consists of a vector with viscoelastic behavior, the contact processes become particularly complex due to the interplay between viscous and elastic effects. The increasing importance of these phenomena in structural and mechanical systems has led to a heightened interest in the study of contact problems. On the other side, quasistatic frictionless contact problems involving Signorini's condition were analyzed for rate-dependent viscoelastic materials in [14, 15], as well as for rate-dependent viscoplastic materials, as detailed in [21] and more recently in [36]. Moreover, the concept of normal compliance in contact conditions was initially presented in [13], focusing on dynamic analyses of elastic and viscoelastic materials. This condition accounts

*Corresponding author.
E-mail address: bolinchenylnu@163.com (B. Chen).
Received 25 July 2025; Accepted 3 June 2026; Published online 10 July 2026.

for the penetration of the body into the obstacle while addressing both the penetration depth and the deformation of surface asperities. Subsequent developments and applications of this condition were discussed in many literature; see, e.g., [2, 10, 27]. Recently, Bouallala et al. [3] investigated the solvability of an innovative mathematical model for contact problems with and without friction, in the context of viscoelasticity with normal compliance. Unlike classical results, their work applied the Kelvin-Voigt constitutive law, enhanced with a fractional time derivative, and extended their analysis to thermoviscoelasticity as detailed in [4]. Results on variational-hemivariational inequalities, particularly regarding their applications to frictional contact problems in viscoelasticity, were provided in [16, 17]. The works [33, 34, 35] make an excellent contribution to the class of variational-hemivariational differential inequalities and quasi-hemivariational inequalities, as well as to their applications. From a numerical standpoint, the normal compliance condition has occasionally been used as a mathematical regularization of Signorini's non-penetration condition and incorporated into numerical solution algorithms. The prevalent techniques for handling contact and friction conditions include the augmented quasi-Lagrangian method [1, 17] and the penalty method [31]. Additionally, the generalized Newton method [22] and a method combining Uzawa's algorithm [25] are frequently used. Nitsche's method [5, 6, 7] and the successive relaxation method with projection [20] are also noteworthy in which we will use such method to establish our numerical results. Furthermore, recent advances in deep learning have spurred rapid growth in data-driven approaches for solving PDEs using deep neural networks (DNNs); see, e.g., [8, 11, 18, 26, 30]. In these approaches, DNNs serve as universal approximators to parameterize the solutions of partial differential equations (PDEs), with the optimal parameters determined by minimizing an optimization problem formulated from the PDE and the associated boundary conditions. The resolution of PDEs using physics-informed neural networks (PINNs) was discussed in [12, 19]. However, the Ritz method was employed for the numerical solution of variational problems [30]. Also, residual neural networks were utilized to approximate evolution operators, facilitating the solution and reconstruction of time-dependent PDEs as detailed in [32]. In [24], Shen et al. proposed a numerical technique by using deep neural networks to address a class of contact problems. They specifically tackled a static frictionless unilateral contact problem by transforming it into a minimization problem. Utilizing a deep neural network to approximate the solution, they successfully resolve this minimization task. The numerical results provided validate the method's effectiveness and accuracy.

In this study, we propose a new approach by using a deep neural network to study a quasistatic unilateral contact problem without friction, for which we establish the existence and uniqueness of a reliable solution. Then, we reformulate the time-discretized problem as an equivalent minimization problem by relaxing the boundary constraints with the addition of two Lagrange terms to the energy function. This transformation enables the reformulation of the original contact problem into a minimization problem, which we address by using a deep neural network. This approach offers the benefits of being unsupervised, not relying on a mesh, and being straightforward to implement. Additionally, we include two numerical experiments that illustrate the effectiveness and precision of our method.

The organization of this paper is as follows. Section 2 presents the model for the quasistatic contact problem involving a viscoelastic body. We start by outlining the foundational material and specifying the assumptions related to the problem data. Next, we derive the variational

formulation of the problem and examine the results concerning the unique solvability of a weak solution. In Section 3, we prove the existence of a weak solution using variational inequalities and fixed-point arguments. Section 4 introduces the deep neural network framework developed for solving discrete minimization problems, including two Lagrange terms in the formulation. Finally, Section 5 showcases two numerical examples to illustrate the effectiveness of the proposed method.

2. Formulation of the Mechanical Problem

Consider a viscoelastic body initially confined within a bounded domain $\Omega \subset \mathbb{R}^2$ and possessing a smooth boundary denoted as $\Gamma = \partial\Omega$. We partition set Γ into three distinct, measurable parts: Γ_D, Γ_N, and Γ_C, with the condition that $meas(\Gamma_D) > 0$. Consider a time interval of interest denoted as $[0,T]$, where T is a positive constant. Let $\mathbb{S}^2$ denote the space of second-order symmetric tensors on $\mathbb{R}^2$. The inner product and corresponding norm on $\mathbb{S}^2$ are given by:

$$\vartheta \cdot \varsigma = \vartheta_i \varsigma_i, \quad \|\varsigma\| = (\varsigma \cdot \varsigma)^{1/2} \quad \text{for all } \vartheta = (\vartheta_i),\ \varsigma = (\varsigma_i) \in \mathbb{R}^2,$$
$$\varpi \cdot \theta = \varpi_{ij}\theta_{ij}, \quad \|\theta\| = (\theta \cdot \theta)^{1/2} \quad \text{for all } \varpi = (\varpi_{ij}),\ \theta = (\theta_{ij}) \in \mathbb{S}^2.$$

For a vector field ς, the normal and tangential components on the boundary Γ are defined as $\varsigma_\nu = \varsigma \cdot \nu$ and $\varsigma_\tau = \varsigma - \varsigma_\nu \nu$, respectively, where ν is the outward unit normal vector on Γ. Likewise, for a tensor field θ, the normal and tangential components are given by $\theta_\nu = (\theta\nu) \cdot \nu$ and $\theta_\tau = \theta\nu - \theta_\nu \nu$, respectively. In this paper, the body is assumed to be fixed on $\Gamma_D \times (0;T)$ and exposed to a volume force ϕ_0 within $\Omega \times (0;T)$, and a traction force density ϕ_N on $\Gamma_N \times (0;T)$. The normalized gap between Γ_C and a rigid foundation is denoted by π. Let $\vartheta : \Omega \times (0,T) \to \mathbb{R}^2$ represent the displacement field, and $\varpi : \Omega \times (0,T) \to \mathbb{R}^2$ the stress tensor. The linearized strain tensor $\varepsilon(\vartheta) = \left(\varepsilon_{ij}(\vartheta)\right)$ is defined as $\varepsilon_{ij}(\vartheta) = \frac{1}{2}\left(\vartheta_{i,j} + \vartheta_{j,i}\right)$, where $\vartheta_{i,j} = \frac{\partial \vartheta_i}{\partial w_j}$. We use "Div" to denote the divergence operator for tensors, i.e., $Div(\varpi) = \left(\varpi_{ij,j}\right)$.

The standard formulation of the contact problem can be stated as follows:

Problem (P) : Find a displacement field $\vartheta : \Omega \times (0,T) \longrightarrow \mathbb{R}^d$ and a stress field $\varpi : \Omega \times (0,T) \longrightarrow \mathbb{S}^d$ such that

$$\varpi(t) = \mathscr{V}\varepsilon\left(\dot{\vartheta}(t)\right) + \mathscr{E}\varepsilon\left(\vartheta(t)\right) \qquad \text{in } \Omega \times (0,T), \tag{2.1}$$
$$Div\left(\varpi(t)\right) + \phi_0(t) = 0 \qquad \text{in } \Omega \times (0,T), \tag{2.2}$$
$$\vartheta(t) = 0 \qquad \text{on } \Gamma_D \times (0,T), \tag{2.3}$$
$$\varpi(t)\nu = \phi_N(t) \qquad \text{on } \Gamma_N \times (0,T), \tag{2.4}$$
$$\vartheta(0,x) = \vartheta_0 \qquad \text{in } \Omega \times (0,T), \tag{2.5}$$
$$\varpi_\tau(t) = 0, \qquad \text{on } \Gamma_C \times (0,T), \tag{2.6}$$
$$\left.\begin{array}{l} \vartheta_\nu(t) \le \pi,\ \ \varpi_\nu(t) + \chi(\vartheta_\nu(t)) \le 0, \\ (\vartheta_\nu(t) - \pi)\left(\varpi_\nu(t) + \chi(\vartheta_\nu(t))\right) = 0 \end{array}\right\} \qquad \text{on } \Gamma_C \times (0,T). \tag{2.7}$$

The following figure presents a concrete illustration of the physical model under study.

Now, we describe each relation of the physical model. Equation (2.1) defines the Kelvin–Voigt viscoelastic constitutive law, where $\mathscr{E} = (e_{ijkl})$ and $\mathscr{V} = (v_{ijkl})$ denote the fourth-order elasticity

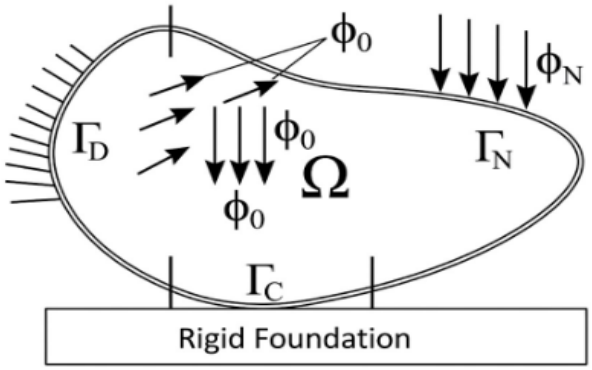

FIGURE 1. Initial configuration of the body at $t = 0$.

and viscosity tensors, respectively. The stress equilibrium is given in equation (2.2). The mechanical boundary conditions are prescribed in equations (2.3)–(2.4), while the initial condition is stated in equation (2.5). Equation (2.6) indicates that the tangential stress vanishes (i.e., no friction force) on the contact boundary Γ_C for all times $t \in (0,T)$, which corresponds to a frictionless contact condition. Finally, equation (2.7) describes the contact with normal compliance and unilateral constraints, combining the Signorini contact condition with a gap and a normal compliance law. For more details, we refer to [9]. To develop the variational formulation of our problem, we first introduce the following functional spaces:

$$M = \left\{\varsigma \in H^1(\Omega)^2 \ : \ \varsigma = 0 \text{ on } \Gamma_D\right\},$$
$$Q = \left\{\theta = (\theta_{ij}) \ : \ \theta_{ij} = \theta_{ji} \in L^2(\Omega)\right\}, \ Q_1 = \left\{\theta \in Q \ : \ Div(\theta) \in L^2(\Omega)\right\}.$$

These are real Hilbert spaces equipped with the following inner products:

$$(\vartheta, \varsigma)_M = \int_\Omega \varepsilon(\vartheta) \cdot \varepsilon(v)\, dx,$$
$$(\varpi, \theta)_Q = \int_\Omega \varpi \cdot \theta \, dx, \ (\varpi, \theta)_{Q_1} = (\varpi, \theta)_Q + (Div(\varpi), Div(\theta))_{L^2(\Omega)^2}.$$

The norms corresponding to the spaces M, Q, and Q_1 are represented by $\|\cdot\|_M$, $\|\cdot\|_Q$, and $\|\cdot\|_{Q_1}$, respectively. We also define the set of admissible displacements as

$$U = \{\varsigma \in M \ : \ \varsigma_\nu \leq \pi \text{ a.e. on } \Gamma_C\},$$

which is a nonempty and closed subset of M. Given that $\text{meas}(\Gamma_D) > 0$, Korn's inequality is applicable in M. Therefore, there exists a constant $c_K > 0$, depending solely on Ω and Γ_D such that, for all $\varsigma \in V$, $\|\varepsilon(\varsigma)\|_Q \geq c_K \|\varsigma\|_{H^1(\Omega)^2}$. By applying the Sobolev trace theorem, there exists a constant c_0, dependent only on Ω, Γ_D, and Γ_C, such that, for all $\vartheta \in M$, $\|\vartheta\|_{L^2(\Gamma_C)^2} \leq c_0 \|\varepsilon(\vartheta)\|_Q$, which indicates that $\|\vartheta\|_M := \|\varepsilon(\vartheta)\|_Q$ is an equivalent norm of M. So, in what follow, we adapt $\|\cdot\|_M$ as the norm of M.

Finally, we use Green's formula in elasticity

$$\int_\Omega \varpi \cdot \varepsilon(\varsigma)\, dx + \int_\Omega \text{Div}(\varpi) \cdot \varsigma \, dx = \int_\Gamma \varpi \nu \cdot \varsigma \, da, \ \forall \varsigma \in H^1(\Omega)^2.$$

Alternatively, we apply the Riesz representation theorem to define the function $f:[0,T]\to V$ through the following expression

$$(\phi(t),\varsigma)_M=\int_{\Gamma_N}\phi_N(t)\cdot\varsigma\,da+\int_\Omega\phi_0(t)\cdot\varsigma\,dx,\ \ \forall\varsigma\in M.$$

We also introduce the functional $j_c:M\times M\to\mathbb{R}$ defined by

$$j_c(\vartheta(t),\varsigma):=\int_{\Gamma_C}\chi\left(\vartheta_\nu(t)\right)\varsigma_\nu\,da,\ \ \forall\varsigma\in M.$$

To simplify, we define the following bilinear forms

$$a:M\times M\to\mathbb{R},\ a(\vartheta,\varsigma):=(\mathscr{E}\varepsilon(\vartheta),\varepsilon(\varsigma))_Q,$$
$$b:M\times M\to\mathbb{R},\ b(\vartheta,\varsigma):=(\mathscr{V}\varepsilon(\vartheta),\varepsilon(\varsigma))_Q,$$

for all $\vartheta,\varsigma\in M$.

We start by outlining the necessary assumptions required for the mathematical analysis of the problem.

(H1) The elasticity tensor $\mathscr{E}=\left(e_{ijkl}\right):\Omega\times\mathbb{S}^2\longrightarrow\mathbb{S}^2$ satisfies:

$$\begin{cases} e_{ijkl}=e_{jikl}=e_{lkij}\in L^\infty(\Omega),\\ \exists m_{\mathscr{E}}>0:e_{ijkl}(x,\zeta)\zeta_k\zeta_l\geq m_{\mathscr{E}}\|\zeta\|^2,\ \forall\zeta\in\mathbb{S}^2,\ \forall x\in\Omega.\end{cases}$$

(H2) The viscosity tensor $\mathscr{V}=\left(\mathscr{V}_{ijkl}\right):\Omega\times\mathbb{S}^d\longrightarrow\mathbb{S}^d$ satisfies:

$$\begin{cases} v_{ijkl}=v_{jikl}=v_{lkij}\in L^\infty(\Omega),\\ \exists m_{\mathscr{V}}>0:v_{ijkl}(x,\zeta)\zeta_k\zeta_l\geq m_{\mathscr{V}}\left\|\zeta\right\|^2,\ \forall\zeta\in\mathbb{S}^2,\ \forall x\in\Omega.\end{cases}$$

(H3) The body forces ϕ_0, surface traction ϕ_1, gap function and initial data enjoy the regularity

$$\phi_0\in W^{1,\infty}\left(0,T;L^2(\Omega)^2\right),\quad \phi_N\in W^{1,\infty}\left(0,T;L^2\left(\Gamma_N\right)^2\right),$$
$$\pi\geq 0,\quad \pi\in L^2(\Gamma_C),\quad \vartheta_0\in M.$$

(H4) The normal compliance function $\chi:\Gamma_C\times\mathbb{R}\to\mathbb{R}_+$ satisfies:

$$\begin{cases} (a)\text{ There exists } L_\chi>0 \text{ such that } \left|\chi\left(x,\vartheta_1\right)-\chi\left(x,\vartheta_2\right)\right|\leq L_\chi\left|\vartheta_1-\vartheta_2\right|,\\ \forall\vartheta_1,\vartheta_2\in\mathbb{R},x\in\Gamma_C,\\ (b)\ \left(\chi(x,\vartheta_1-\chi(x,\vartheta_2)\left(\vartheta_1-\vartheta_2\right)\geq 0,\ \forall x\in\Gamma_C,\ \forall\vartheta_1,\vartheta_2\in\mathbb{R}.\\ (c)\ \chi(x,\vartheta)=0\,\forall\vartheta\leq 0\text{ and }x\in\Gamma_C.\end{cases}$$

By $(H2)$, there exists a constant $\exists M_{\mathscr{E}}>0$ such that $|a(\vartheta,\varsigma)|\leq M_{\mathscr{E}}\|\vartheta\|_M\|\varsigma\|_M$ for all $\vartheta,\varsigma\in M$. $(h4)$(b) points out that χ is monotone with respect to the second variable.

We can now formulate our weak problem. To do so, let ϑ and ϖ be sufficiently regular functions satisfying (2.1)-(2.7). Let $\varsigma\in U$. We multiply equation (2.2) by $(\varsigma-\vartheta(t))$ and integrate the resulting over Ω to get:

$$\int_\Omega Div(\varpi(t))\cdot(\varsigma-\vartheta(t))\,dx+\int_\Omega\phi_0\cdot(\varsigma-\vartheta(t))\,dx=0.$$

Using Green's formula, we obtain

$$\begin{aligned}&\int_\Gamma \varpi(t)\nu\cdot(\varsigma-\vartheta(t))\,da+\int_\Omega \phi_0(t)\cdot(\varsigma-\vartheta(t))\,dx\\&\quad=\int_\Omega \varpi(t)\cdot(\varepsilon(\varsigma)-\varepsilon(\vartheta(t)))dx.\end{aligned}\tag{2.8}$$

Since Γ_D, Γ_N, and Γ_C form a partition of Γ, considering (2.3)–(2.4) and (2.6), we have

$$\begin{aligned}&\int_\Gamma \varpi(t)\nu\cdot(\varsigma-\vartheta(t))\,da\\&\quad=\underbrace{\int_{\Gamma_D}\varpi(t)\nu\cdot(\varsigma-\vartheta(t))\,da}_{=0}+\int_{\Gamma_N}\varpi(t)\nu\cdot(\varsigma-\vartheta(t))\,da\\&\qquad+\int_{\Gamma_C}\varpi(t)\nu\cdot(\varsigma-\vartheta(t))\,da\\&\qquad\quad=\int_{\Gamma_N}\phi_1(t)\cdot(\varsigma-\vartheta(t))\,da+\int_{\Gamma_C}(\varpi_\tau(t)+\varpi_\nu(t)\nu)\cdot(\varsigma-\vartheta(t))\,da\\&\qquad\qquad=\int_{\Gamma_N}\phi_1(t)\cdot(\varsigma-\vartheta(t))\,da+\underbrace{\int_{\Gamma_C}\varpi_\tau(t)\cdot(\varsigma_\tau-\vartheta_\tau(t))\,da}_{=0}\\&\qquad\qquad+\int_{\Gamma_C}\varpi_\nu(t)(\varsigma_\nu-\vartheta_\nu(t))\,da.\end{aligned}\tag{2.9}$$

Considering the contact condition (2.7), we have

$$\begin{aligned}\varpi_\nu(t)\,(\varsigma_\nu-\vartheta_\nu(t))&=\underbrace{(\varpi_\nu(t)+\chi\,(\vartheta_\nu(t)))\,(\varsigma_\nu-\pi)}_{\geq 0}\\&+\underbrace{(\varpi_\nu(t)+\chi\,(\vartheta_\nu(t)))\,(\pi-\vartheta_\nu(t))}_{=0}-\chi\,(\vartheta_\nu(t))\,(\varsigma_\nu-\vartheta_\nu(t))\quad\text{a.e. on }\Gamma_C.\end{aligned}$$

Thus $\varpi_\nu(t)\,(\varsigma_\nu-\vartheta_\nu(t))\geq-\chi\,(\vartheta_\nu(t))\,(\varsigma_\nu-\vartheta_\nu(t))$, which yields

$$\int_{\Gamma_C}\varpi_\nu(t)\,(\varsigma_\nu-\vartheta_\nu(t))\,da\geq-\int_{\Gamma_C}\chi\,(\vartheta_\nu(t))\,(\varsigma_\nu-\vartheta_\nu(t))\,da.\tag{2.10}$$

Combining (2.8) and (2.9) with (2.10), we deduce that

$$\begin{aligned}&\int_\Omega \varpi(t)\cdot(\varepsilon(\varsigma)-\varepsilon(\vartheta(t)))\,dx+\int_{\Gamma_C}\chi\,(\vartheta_\nu(t))\,(\varsigma_\nu-\vartheta_\nu(t))\,da\\&\quad\geq\int_{\Gamma_N}\phi_N(t)\cdot(\varsigma-\vartheta(t))\,da+\int_\Omega\phi_0(t)\cdot(\varsigma-\vartheta(t))\,dx.\end{aligned}$$

Finally, we obtain the variational formulation of **Problem (P)** as follows.

Problem (PV) : Find a displacement field $\vartheta:\Omega\times(0,T)\longrightarrow\mathbb{R}^2$ and a stress field $\varpi:\Omega\times(0,T)\longrightarrow\mathbb{S}^2$ such that, for a.e. $t\in(0,T)$ and for all $\varsigma\in M$,

$$\begin{aligned}&a(\vartheta(t),\varsigma-\vartheta(t))+b(\dot\vartheta(t),\varsigma-\vartheta(t))+j_c(\vartheta(t),\varsigma-\vartheta(t))\geq(\phi(t),\varsigma-\vartheta(t))_M,\\&\varpi(t)=\mathscr{V}\varepsilon\left(\dot\vartheta(t)\right)+\mathscr{E}\varepsilon\left(\vartheta(t)\right),\\&\vartheta(x,0)=\vartheta_0.\end{aligned}$$

3. An Existence and Uniqueness result

Indeed, the existence and uniqueness of **Problem (PV)** was established in [33, 34, 35] by using a surjectivity theorem and monotonicity arguments. However, in this paper, we recall the unique solvability result for **Problem (PV)** and give an alternative proof of the existence and uniqueness of **Problem (PV)**. More precisely, we apply Banach fixed point theorem together with Lax-Milgram theorem to obtain the desired conclusion.

Theorem 3.1. *Under the assumptions (H1)–(H4),* ***Problem (PV)*** *admits a unique solution, which adheres to the following regularity conditions:* $\vartheta \in W^{2,\infty}(0,T;M)$ *and* $\varpi \in W^{2,\infty}(0,T;Q_1)$.

The proof of Theorem 3.1 is structured in several steps, utilizing variational inequalities and the Banach fixed-point theorem. Given $\lambda \in W^{1,\infty}(0,T;M)$, we consider the following auxiliary variational problem.

Problem (PVOX) : Find a displacement field $\vartheta_\lambda : \Omega \times (0,T) \longrightarrow \mathbb{R}^2$, for all $t \in [0,T]$ and $\varsigma \in M$ such that

$$\begin{aligned} &a(\vartheta_\lambda(t), \varsigma - \vartheta_\lambda(t)) + b(\dot{\vartheta}_\lambda(t), \varsigma - \vartheta_\lambda(t)) + (\lambda(t), \varsigma - \vartheta_\lambda(t))_M \\ &\quad \geq (\phi(t), \varsigma - \vartheta_\lambda(t))_M, \\ &\vartheta_\lambda(x,0) = \vartheta_0. \end{aligned} \tag{3.1}$$

Lemma 3.1. *A unique solution* ϑ_λ *for* ***Problem (PVOX)*** *can be found, and it is such that* $\vartheta_\lambda \in W^{2,\infty}(0,T;M)$.

Proof. We proceed by introducing an auxiliary function and the Riesz representation theorem. For almost every $t \in [0,T]$, we define $\phi_\lambda(t) \in M$ such that

$$(\phi_\lambda(t), \varsigma - \vartheta_\lambda(t))_M = (\phi(t), \varsigma - \vartheta_\lambda(t))_M - (\lambda(t), \varsigma - \vartheta_\lambda(t))_M, \quad \forall \varsigma \in M.$$

This definition ensures that the right-hand side of the variational formulation can be written in a compact form. Consequently, inequality (3.1) can be rewritten as

$$a(\vartheta_\lambda(t), \varsigma - \vartheta_\lambda(t)) + b\left(\dot{\vartheta}_\lambda(t), \varsigma - \vartheta_\lambda(t)\right) \geq (\phi_\lambda(t), \varsigma - \vartheta_\lambda(t))_M.$$

Under assumption (H1), one sees that $a(\cdot,\cdot)$ is continuous. Moreover, by assumption (H2), $b(\cdot,\cdot)$ is continuous and coercive. Since $\lambda \in W^{1,\infty}(0,T;M)$ and $\phi \in W^{1,\infty}(0,T;M)$, it follows that $\phi_\lambda \in W^{1,\infty}(0,T;M)$. Finally, by applying [28, Corollary 4.4], we deduce that **Problem (PVOX)** admits a unique solution. □

In the second step, we define the $\Phi : W^{1,\infty}(0,T;M) \to W^{1,\infty}(0,T;M)$ by

$$(\Phi\lambda(t), \varsigma)_M := j_c(\vartheta_\lambda(t), \varsigma), \ \forall \varsigma \in M, \ t \in [0,T]. \tag{3.2}$$

We proceed with the following fixed-point result.

Lemma 3.2. *The operator* Φ *has a unique fixed point* $\lambda^* \in W^{1,\infty}(0,T;M)$.

Proof. Let $\lambda_1, \lambda_2 \in W^{1,\infty}(0,T;M)$. From hypothses (H4) and (3.2), we can see that

$$\|\Phi\lambda_1(t) - \Phi\lambda_2(t)\|_M \leq L_\chi c_0^2 \left\|\vartheta_{\lambda_1}(t) - \vartheta_{\lambda_2}(t)\right\|_M. \tag{3.3}$$

Employing (3.1) and performing algebraic manipulations, we obtain

$$\begin{aligned} &a\left(\vartheta_{\lambda_2}(t) - \vartheta_{\lambda_1}(t), \vartheta_{\lambda_2}(t) - \vartheta_{\lambda_1}(t)\right) \\ &\leq b\left(\dot{\vartheta}_{\lambda_2}(t) - \dot{\vartheta}_{\lambda_1}(t), \vartheta_{\lambda_2}(t) - \vartheta_{\lambda_1}(t)\right) + \left(\lambda_1(t) - \lambda_2(t), \vartheta_{\lambda_2}(t) - \vartheta_{\lambda_1}(t)\right)_M, \quad \forall t \in [0,T]. \end{aligned}$$

Based on assumptions (H1), it follows that

$$m_{\mathscr{E}}\|\vartheta_{\lambda_2}(t)-\vartheta_{\lambda_1}(t)\|_M^2 \leq \frac{d}{dt}\frac{1}{2}\left(b\left(\vartheta_{\lambda_2}(t)-\vartheta_{\lambda_1}(t),\vartheta_{\lambda_2}(t)-\vartheta_{\lambda_1}(t)\right)\right) + \|\lambda_1(t)-\lambda_2(t)\|_M\left\|\vartheta_{\lambda_2}(t)-\vartheta_{\lambda_1}(t)\right\|_M. \tag{3.4}$$

Starting from inequality (3.4), we integrate both sides over the interval $[0,t]$. Thus

$$m_{\mathscr{E}}\int_0^t \|\vartheta_{\lambda_2}(s)-\vartheta_{\lambda_1}(s)\|_M^2\,ds \leq \int_0^t \frac{d}{ds}\frac{1}{2}\left(b\big(\vartheta_{\lambda_2}(s)-\vartheta_{\lambda_1}(s),\vartheta_{\lambda_2}(s)-\vartheta_{\lambda_1}(s)\big)\right)ds + \int_0^t \|\lambda_1(s)-\lambda_2(s)\|_M\left\|\vartheta_{\lambda_2}(s)-\vartheta_{\lambda_1}(s)\right\|_M ds.$$

Using the fundamental theorem of calculus, it follows that

$$\begin{aligned} m_{\mathscr{E}}\int_0^t \|\vartheta_{\lambda_2}(s)-\vartheta_{\lambda_1}(s)\|_M^2\,ds \quad &\leq \frac{1}{2}b\big(\vartheta_{\lambda_2}(t)-\vartheta_{\lambda_1}(t),\vartheta_{\lambda_2}(t)-\vartheta_{\lambda_1}(t)\big) \\ &\quad -\frac{1}{2}b\big(\vartheta_{\lambda_2}(0)-\vartheta_{\lambda_1}(0),\vartheta_{\lambda_2}(0)-\vartheta_{\lambda_1}(0)\big) \\ &\quad +\int_0^t \|\lambda_1(s)-\lambda_2(s)\|_M\left\|\vartheta_{\lambda_2}(s)-\vartheta_{\lambda_1}(s)\right\|_M ds. \end{aligned}$$

Since $\vartheta_{\lambda_2}(0)=\vartheta_{\lambda_1}(0)=\vartheta_0$, we have $\vartheta_{\lambda_2}(0)-\vartheta_{\lambda_1}(0)=0$. Therefore,

$$b\big(\vartheta_{\lambda_2}(0)-\vartheta_{\lambda_1}(0),\vartheta_{\lambda_2}(0)-\vartheta_{\lambda_1}(0)\big)=0.$$

Hence,

$$\frac{1}{2}b\big(\vartheta_{\lambda_2}(t)-\vartheta_{\lambda_1}(t),\vartheta_{\lambda_2}(t)-\vartheta_{\lambda_1}(t)\big) \leq \int_0^t \|\lambda_1(s)-\lambda_2(s)\|_M\left\|\vartheta_{\lambda_2}(s)-\vartheta_{\lambda_1}(s)\right\|_M ds.$$

Using the continuity and coercivity of the operator b, there exists a positive constant $c>0$ such that

$$\|\vartheta_{\lambda_2}(t)-\vartheta_{\lambda_1}(t)\|_M^2 \leq c\int_0^t \|\lambda_1(s)-\lambda_2(s)\|_M\left\|\vartheta_{\lambda_2}(s)-\vartheta_{\lambda_1}(s)\right\|_M ds.$$

Finally, by applying the Cauchy–Schwarz inequality, we deduce

$$\|\vartheta_{\lambda_2}(t)-\vartheta_{\lambda_1}(t)\|_M^2 \leq c\left\{\int_0^t \left\|\vartheta_{\lambda_2}(s)-\vartheta_{\lambda_1}(s)\right\|_M^2 ds+\int_0^t \|\lambda_1(s)-\lambda_2(s)\|_M^2\,ds\right\}.$$

Applying Gronwall's lemma, it turns out

$$\|\vartheta_{\lambda_2}(t)-\vartheta_{\lambda_1}(t)\|_M^2 \leq c\int_0^t \|\lambda_1(s)-\lambda_2(s)\|_M^2\,ds. \tag{3.5}$$

By integrating (3.3) and (3.5), we infer that

$$\|\Phi\lambda_1(t)-\Phi\lambda_2(t)\|_M \leq c\int_0^t \|\lambda_2(s)-\lambda_1(s)\|_M ds, \quad \forall t\in[0,T].$$

Reiterating this inequality n times leads to

$$\|\Phi^n\lambda_1(t)-\Phi^n\lambda_2(t)\|_M \leq \frac{c^nT^n}{n!}\int_0^t \|\lambda_2(s)-\lambda_1(s)\|_M ds.$$

This indicates that, for sufficiently large n with $\frac{c^nT^{n+1}}{n!}<1$, operator Φ^n acts as a contraction map on $W^{1,\infty}(0,T;M)$. Consequently, there exists a unique $\lambda^*\in W^{1,\infty}(0,T;M)$ such that $\Phi^n\lambda^*=\lambda^*$, making λ^* the unique fixed point of Φ. □

We are now prepared to prove the theorem.

Proof of Theorem 3.1. **Existence.** Let $\lambda^* \in W^{1,\infty}(0,T;M)$ be the unique fixed point of Φ, and let ϑ_{λ^*} be the unique solution to **Problem (PVOX)** with $\lambda = \lambda^*$. It can observe that ϑ_{λ^*} is a solution to **Problem (PV)**. In fact, defining $\varpi^*(t) = \mathscr{V}\varepsilon\left(\dot{\vartheta}^*(t)\right) + \mathscr{E}\varepsilon\left(\vartheta^*(t)\right)$ and useing (3.2) as well as $\Phi(\lambda^*) = \lambda^*$, it follows that $(\vartheta^*, \varpi^*) \in W^{2,\infty}(0,T;M) \times W^{2,\infty}(0,T;Q_1)$ satisfies **Problem (PV)**.

Uniqueness. The uniqueness aspect of Theorem 3.1 is established through reasoning akin to that found in [29]. It directly results from the uniqueness of the fixed point of the operator Φ, as described in (3.2). □

4. Deep Neural Network for Discrete Optimization Problem

In this section, we introduce a deep learning framework designed to address the contact problem discussed earlier. Our method features two key components:

i) A neural network architecture for defining the objective function;
ii) A loss function derived from the contact problem.

The objective is to train a deep neural network $\vartheta_\varphi(x)$ to approximate the displacement field $\vartheta(x)$ across all x in Ω, where φ denotes the trainable parameters of the network, including weights and biases. The architecture of the model consists of a neural network with ten fully connected layers, each followed by a LeakyReLU activation function, specified as:

$$\beta(x) = \begin{cases} x & \text{if } x \geq 0, \\ ax & \text{if } x < 0. \end{cases}$$

In this function, a is a small positive constant, with $a = 0.1$ being used by default.
Input: The model handles two-dimensional data, typically represented as a 3-dimensional vector (x_1, x_2, t).
Hidden Layers: Each fully connected hidden layer comprises 64 neurons and is followed by a LeakyReLU activation function with a slope coefficient of 0.1.
Output Layer: The final dense layer contains 2 output neurons, which generate the model's final outputs ϑ_φ^1 and ϑ_φ^2.

We consider the time interval $[0,T]$ partitioned into points $0 < t_0 < t_1 < \cdots < t_N = T$, with step sizes denoted by $\delta t_n = t_n - t_{n-1}$ for $n = 1,2,\ldots,N$. For the sequence $\{\vartheta_n\}_{n=0}^N$, we define $\delta\vartheta_n = \frac{\vartheta_n - \vartheta_{n-1}}{\delta t_n}$.

The semi-discrete approximation method via using the backward Euler scheme is given by:
Problem (PVD) : Find a a sequence $\{\vartheta_n\}$ such that, for all $\varsigma \in V$,

$$\begin{aligned} &a(\vartheta_n, \varsigma - \vartheta_n) + b(\delta\vartheta_n, \varsigma - \vartheta_n) + j_c(\vartheta_n, \varsigma - \vartheta_n) \geq (\phi_n, \varsigma - \vartheta_n)_M, \\ &\vartheta_n(x) = \vartheta_0, \end{aligned}$$

where $\phi_n = \phi(t_n)$.

According to the research in [23, 24], we reformulate the problem as a minimization problem by incorporating two Lagrange multipliers. Specifically, the problem is expressed as

$$\min_{\varsigma \in H^1(\Omega)} E(\varsigma) = \frac{1}{2}\tilde{a}(\varsigma,\varsigma) + j_c(\varsigma,\varsigma) - (\tilde{\phi},\varsigma)_M + \alpha_1 \int_{\Gamma_D} |\varsigma|^2\, dx + \alpha_2 \int_{\Gamma_C} \max(0, \varsigma - \pi)\, dx,$$

with

$$\tilde{a}(\varsigma,\varsigma) = a(\varsigma,\varsigma) + \frac{1}{\delta t_n} b(\varsigma,\varsigma),\ (\tilde{\phi},\varsigma)_M = (\phi,\varsigma) + \frac{1}{\delta t_n} b(\vartheta_{n-1},\varsigma).$$

Additionally, α_1 and α_2 represent the weights associated with the Lagrange multipliers. To address the problem described, we employ deep neural networks as follows:

$$\min_{\varphi} L(\varphi) = \frac{1}{2}\tilde{a}(\vartheta^{\varphi},\vartheta^{\varphi}) + j_c(\vartheta^{\varphi},\vartheta^{\varphi}) - (\tilde{\phi},\vartheta^{\varphi})_M + \alpha_1 \int_{\Gamma_D} |\vartheta^{\theta}|^2 dx + \alpha_2 \int_{\Gamma_C} \max(0,\vartheta_{\nu}^{\varphi} - \pi)\, dx.$$

We then present the discrete version of L as $\min_{\varphi} \hat{L}(\varphi) = \hat{L}_{\text{main}}(\varphi) + \hat{L}_{\text{lagrange}}(\varphi)$, where

$$\hat{L}_{\text{main}}(\varphi) = \frac{1}{2N_\Omega}\sum_{i=1}^{N_\Omega} (\mathscr{E}\varepsilon(\vartheta_i^{\varphi}))\cdot\varepsilon(\vartheta_i^{\varphi}) + \frac{1}{2\delta t N_\Omega}\sum_{i=1}^{N_\Omega} (\mathscr{V}\varepsilon(\vartheta_i^{\varphi}))\cdot\varepsilon(\vartheta_i^{\varphi}) + \frac{1}{N_C}\sum_{i=1}^{N_C} \chi(\vartheta_{\nu,i}^{\varphi})\cdot\vartheta_{\nu,i}^{\varphi}(t) - \frac{1}{N_N}\sum_{i=1}^{N_N}(\phi_N\cdot\vartheta_i^{\varphi}) - \frac{1}{N_\Omega}\sum_{i=1}^{N_\Omega}(\phi_0\cdot\vartheta_i^{\varphi}),$$

and

$$\hat{L}_{\text{lagrange}}(\varphi) = \alpha_1 \frac{1}{N_D}\sum_{i=1}^{N_D} \left\|\vartheta_i^{\varphi}\right\|^2 + \alpha_2 \frac{1}{N_C}\sum_{i=1}^{N_C} \max(0,\vartheta_{\nu,i}^{\varphi} - \pi),$$

where ϑ_i^{φ} denotes the value at the i-th sampled point, and N_Ω, N_D, N_N, N_C represent the number of sampled points in the domain Ω, and on the boundaries Γ_D, Γ_N, and Γ_C, respectively. Furthermore, $\vartheta_{\nu}^{\varphi}$ indicates the outward normal component.

5. Numerical Simulations and Experiments

In this section, we illustrate the effectiveness and precision of the proposed method using a numerical example. We examine a two-dimensional rectangular domain $\Omega = (0,2)\times(0,1)$ with the boundaries

$$\Gamma_D = \{0\}\times[0,1],\quad \Gamma_C = [0,2]\times\{0\},\quad \Gamma_N = [0,2]\times\{1\}\cup\{2\}\times[0,1].$$

The function $\chi(\cdot)$ is defined as $\chi(r) = c_\nu[r]^+$, where $c_\nu = 10\ GPa$ is the stiffness coefficient of the foundation. The elasticity tensor operator $\mathscr{E}$ is given by

$$(\mathscr{E}\tau)_{ij} = \frac{E\times\kappa}{1-\kappa^2}(\tau_{11}+\tau_{22})\delta_{ij} + \frac{E}{1+\kappa}\tau_{ij},\quad 1\le i,j\le 2,\quad \forall\tau\in\mathbb{S}^2$$

where the Young's modulus $E = 1000\ N/m^2$ and the Poisson's ratio of the material $\kappa = 0.4$. The viscosity tensor operator $\mathscr{V}$ is given by

$$(\mathscr{V}\tau)_{ij} = \mu_1(\tau_{11}+\tau_{22})\delta_{ij} + \mu_2\tau_{ij},\quad 1\le i,j\le 2,\quad \forall\tau\in\mathbb{S}^2.$$

The material constants $\mu_1 = 0.25$ and $\mu_2 = 0.5$ are parameters that characterize the viscoelastic behavior of the material. The volumetric and surface forces are

$$\phi_0 = (0,0)\,\text{N/m}^2,\ \ \phi_N = \begin{cases} (0,-10t)\,\text{N/m}^2 & \text{on } [0,2]\times\{1\},\\ (0,0)\,\text{N/m}^2 & \text{on } \{2\}\times[0,1].\end{cases}$$

The following figure shows the body at time $t = 0$ without any applied forces. Figures 3(a) and 3(b) show the deformed configuration and the distribution of the Von Mises effective stress

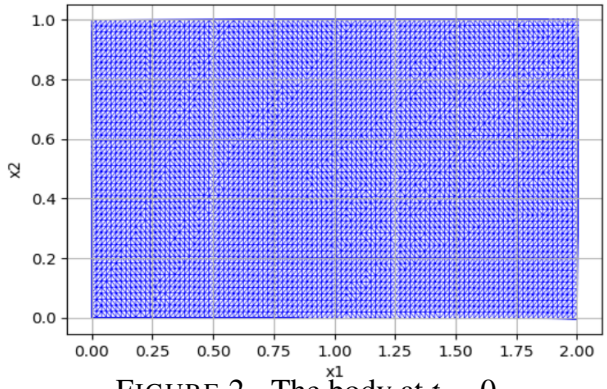

FIGURE 2. The body at $t = 0$.

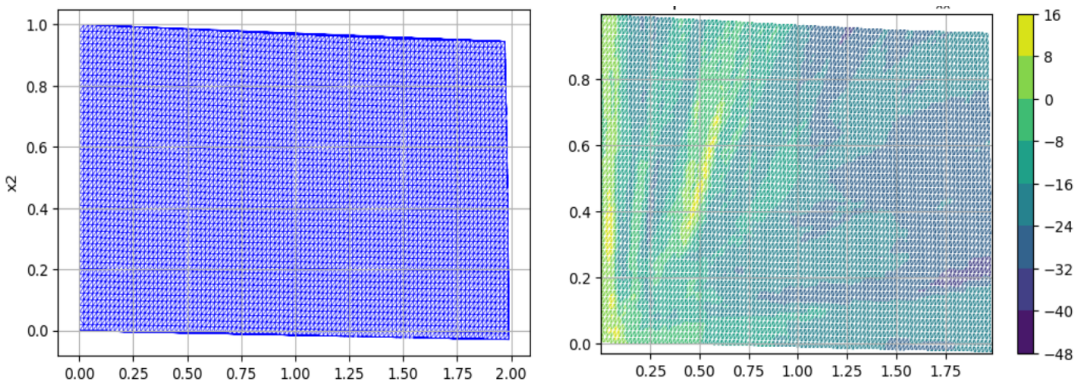

(a) (b)

FIGURE 3. (a) Deformed configuration. (b) Deformed configuration with Von Mises effective stress distribution.

at $t = 0.1$ and $\pi = 0.05$, respectively. The deformed configuration reflects the global displacement predicted by the Kelvin–Voigt model, where both elastic and viscous effects contribute to the deformation. The Von Mises stress distribution highlights localized stress concentrations, especially near the boundary and contact regions. These results are consistent with the unilateral contact formulation, showing how the model captures the interaction between deformation and stress transmission in the body. Figures 4(a) and 4(b) depict the distribution of normal displacements and normal stresses in the contact region at $t = 0.1$ and $\pi = 0.05$, respectively. Figures 4(a) and 4(b) illustrate the evolution along the contact boundary Γ_C.

The normal displacements decrease monotonically, indicating progressive compression of the body against the foundation. The normal stresses are predominantly negative, showing that the contact is mainly compressive, consistent with unilateral contact conditions. Some oscillations in the stress distribution reflect local variations in the contact response and numerical effects. Overall, the results are physically consistent with a frictionless contact model under increasing loading.

We will conduct a second simulation at $t = 0.5$ and $\pi = 0.1$. Figures 5(a) and 5(b) illustrate the deformed configuration and the distribution of the Von Mises effective stress. In comparison, Figures 6(a) and 6(b) highlight the distribution of normal displacements and normal stresses on Γ_C.

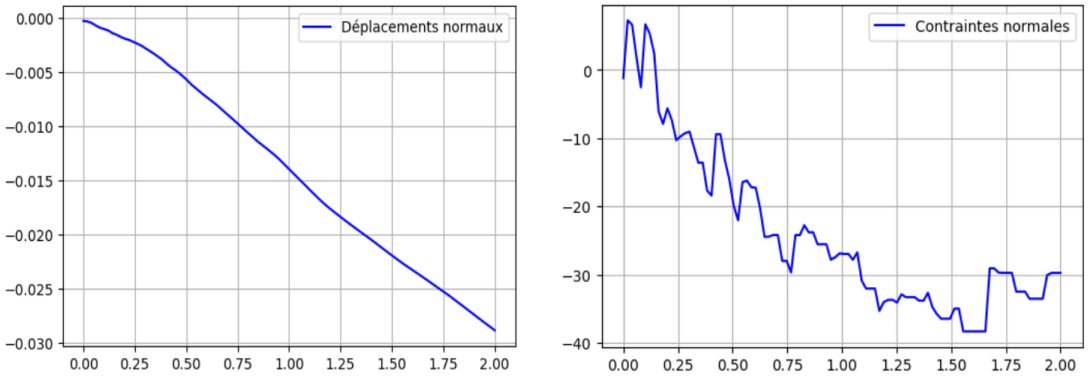

(a) (b)

FIGURE 4. (a) Normal displacements on Γ_C. (b) Normal stresses on Γ_C.

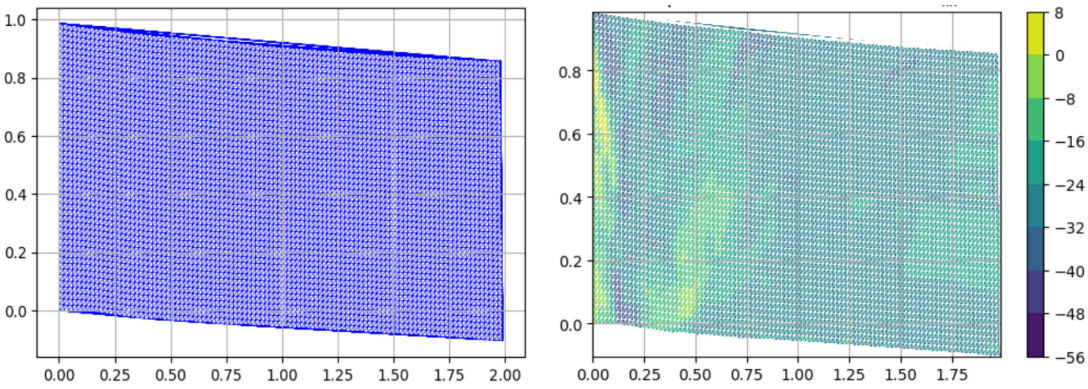

(a) (b)

FIGURE 5. (a) Deformed configuration. (b) Deformed configuration with Von Mises effective stress distribution.

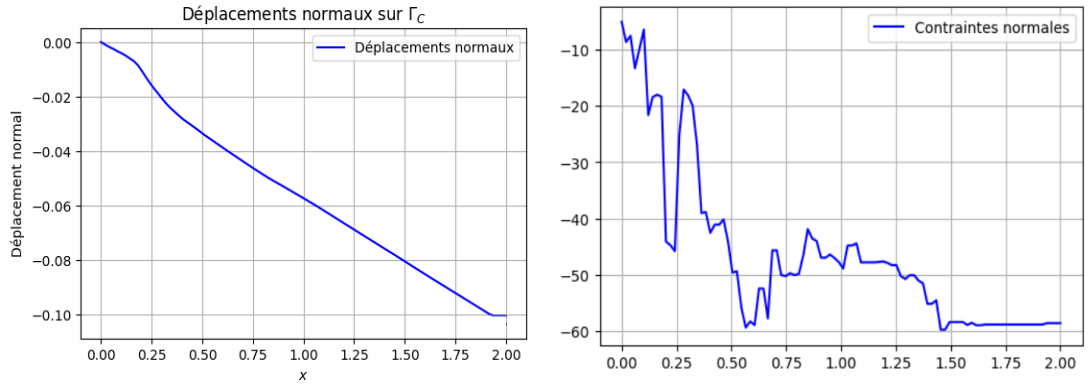

(a) (b)

FIGURE 6. (a) Normal displacements on Γ_C. (b) Normal stresses on Γ_C.

Figures 5(a) and 5(b) show a deformed configuration with predominantly negative displacements (ranging from -56 to 8) and localized von Mises stress concentrations, indicating locally nonlinear mechanical behavior. Figures 6(a) and 6(b) specify, on the interface Γ_C, normal displacements ranging from -60 to -10 and essentially negative normal stresses, signifying dominant compression with a few local tensile points. Together, these results reveal a strong

interaction between deformation and stress at the interface, typical of contact problems or initial gap loading.

6. Conclusion

In this research, we examined a quasi-static unilateral contact problem without friction. We started by formulating its weak formulation and demonstrating its unique solvability. Subsequently, we established that this weak formulation can be represented as a minimization problem. Utilizing this minimization problem, we constructed a deep learning framework to solve the contact issue. Numerical tests confirm the efficacy and precision of our method.

Our approach is advantageous as it is unsupervised, does not require a mesh, and is easy to implement. It shows potential for addressing more complex contact scenarios, and we aim to explore additional contact problems in future studies. A limitation of our approach is the need to retrain the deep neural networks for different elastic and viscoelastic layer thicknesses. Although transfer learning can speed up training, it remains time-consuming and requires substantial fine-tuning.

In future research, we plan to compare our method with other well-established techniques, such as finite element methods, and evaluate algorithms like augmented Lagrangian, penalization, and ADMM.

Acknowledgements
This work was supported by the National Natural Science Foundation of Guangxi under Grant Nos. 2026GXNSFAA00640110 and 2026GXNSFHA00640378.

References

[1] P. Alart, A. Curnier, A mixed formulation for frictional contact problems prone to Newton like solution methods, Comput. Meth. Appl. Mech. Eng. 92 (1991), 353-375.
[2] S. Bordas, P. Nguyen, Y. Zhang, A computational framework for normal compliance contact in viscoelastic materials using the finite element method, Comput. Meth. Appl. Mech. Eng. 411 (2023), 115056.
[3] M. Bouallala, EL-H. Essoufi, V. T. Nguyen, W. Pang, A time-fractional of a viscoelastic frictionless contact problem with normal compliance, Eur. Phys. J. Special Topics 232 (2023), 2549–2558.
[4] M. Bouallala, E. H. Essoufi, A thermo-viscoelastic fractional contact problem with normal compliance and coulomb's friction, J. Mat. Phys. Anal. Geometry, 17 (2021), 280-294.
[5] F. Chouly, P. Hild, A Nitsche-base method for unilateral contact problems : numerical analysis, SIAM J. Numer. Anal. 51 (2012), 1295-1307.
[6] F. Chouly, P. Hild, Y. Renard, A Nitsche finite element method for dynamic contact: 1. Space semi-discretization and time-marching schemes, ESAIM: Math. Model. Numer. Anal. 49 (2015), 481-502.
[7] F. Chouly, P. Hild, Y. Renard, Symmetric and non-symmetric variants of Nitsche's method for contact problems in elasticity: theory and numerical experiments, Math. Comput. 84 (293) (2015), 1089-1112.
[8] J. Han, A. Jentzen, E. Weinan, Overcoming the curse of dimensionality: Solving high-dimensional partial differential equations using deep learning, Proc. Nat. Acad. Sci. 115 (2018), 8505-8510.
[9] J. Jarušek, M. Sofonea, On the solvability of dynamic elastic-visco-plastic contact problems, ZAMM J. Appl. Math. Mech. 88 (2008), 3-22.
[10] Q. Liu, T. Yin, Numerical treatment of normal compliance contact problems in viscoelasticity, J. Comput. Phys. 451 (2022), 110883.
[11] Z. Long, Y. Lu, B. Dong, PDE-Net 2.0: Learning PDEs from data with a numeric-symbolic hybrid deep network, J. Comput. Phys. 399 (2019), 108925.
[12] L. Lu, et al., DeepXDE: A deep learning library for solving differential equations, SIAM Rev. 63 (2021), 208-228.

[13] J. A. C. Martins, J. T. Oden, Existence and uniqueness results for dynamic contact problems withnonlinear normal and friction interface laws, Nonlinear Anal. 11 (1987), 407-428.
[14] A. Matei, S. Sitzmann, K. Willner, B. I. Wohlmuth, A mixed variational formulation for a class of contact problems in viscoelasticity, Appl. Anal. 97 (2018), 1340-1356.
[15] S. Migórski, D. Paczka, Variational inequality with almost history-dependent operator for frictionless contact problems, J. Math. Anal. Appl. 485 (2020), 123803.
[16] S. Migórski, Y. Bai, S. Zeng, A class of generalized mixed variational-hemivariational inequalities II: Applications, Nonlinear Anal. 50 (2019), 633-650.
[17] S. Migórski, S. Zeng, Rothe method and numerical analysis for history-dependent hemivariational inequalities with applications to contact mechanics, Numer. Algo. 82 (2019), 423-450.
[18] M. Raissi, P. Perdikaris, G. E. Karniadakis, Physics-informed neural networks: A deep learning framework for solving forward and inverse problems involving nonlinear partial differential equations, J. Comput. Phys. 378 (2019), 686-707.
[19] M. Raissi, P. Perdikaris, G. E. Karniadakis, Physics-informed neural networks: A deep learning framework for solving forward and inverse problems involving nonlinear partial differential equations, J. Comput. Phys. 378 (2019), 686-707.
[20] M. Raous, Quasistatic Signorini Problem with Coulomb Friction and Coupling to Adhesion. In: P. Wriggers, P. Panagiotopoulos, (eds) New Developments in Contact Problems. International Centre for Mechanical Sciences, vol 384. Springer, Vienna, 1999.
[21] M. Rochdi, M. Sofonea, On frictionless contact between two elastic-viscoplastic bodies, Q. J. Mech. Appl. Math. 50 (1997), 481-496.
[22] Y. Renard, Generalized Newton's methods for the approximation and resolution of frictional contact problems in elasticity, Comput. Meth. Appl. Mech. Eng. 256 (2013), 38-55.
[23] M. Rong, D. Zhang, N. Wang, A Lagrangian dual-based theory-guided deep neural network, Complex and Intelligent Systems, 8 (2022), 4849-4862.
[24] X. Shen, X. Cheng, K. Liang, X. Wang, Z. Wu, A deep neural network-based numerical method for solving contact problems, J. Nonlinear Var. Anal. 6 (2022), 483-498.
[25] J.C. Simo, T.A. Laursen, An augmented Lagrangian treatment of contact problems involving friction, Comput. Structures 42 (1992), 97-116.
[26] J. Sirignano, K. Spiliopoulos, DGM:A deep learning algorithm for solving partial differential equations, J. Comput. Phys. 375 (2018), 1339-1364.
[27] M. Sofonea, Y. Xiao, M. Couderc, Optimization problems for a viscoelastic frictional contact problem with unilateral constraints, Nonlinear Anal. 50 (2019), 86-103.
[28] M. Sofonea, A. Matei, Variational Inequalities with Applications, A Study of Antiplane Frictional Contact Problems, Springer New York, 2009. doi: 10.1007/978-0-387-87460-9
[29] M. Sofonea, On a contact problem for elastic-viscoplastic bodies, Nonlinear Anal. 29 (1997), 1037-1050.
[30] E. Weinan, B. Yu, The deep Ritz method: a deep learning-based numerical algorithm for solving variational problems, Commun. Math. Statis. 6 (2018), 1-12.
[31] P. Wriggers, Computational Contact Mechanics, Wiley, Chichester, 2002.
[32] K. Wu, D. Xiu, Data-driven deep learning of partial differential equations in modal space, J. Comput. Phys. 408 (2020), 109307.
[33] S.D. Zeng, S. Migórski, Z.H. Liu, Well-posedness, optimal control, and sensitivity analysis for a class of differential variational-hemivariational inequalities, SIAM J. Optim. 31 (2021), 2829-2862.
[34] S.D. Zeng, A.A. Khan, S. Migorski, A new class of generalized quasi-variational inequalities with applications to Oseen problems under nonsmooth boundary conditions, Sci. China Math. 67 (2024), 315-338.
[35] S.D. Zeng, S. Migórski, A.A. Khan, Nonlinear quasi-hemivariational inequalities: Existence and optimal control, SIAM J. Control Optim. 59 (2021), 1246-1274.
[36] X. Zhou, L. Wei, Quasistatic contact problems for rate-dependent viscoplastic materials: An analytical and numerical study, J. Comput. Phys. 457 (2023), 111-128.